ChemComm

Cite this: *Chem. Commun.*, 2011, **47**, 10479–10481

www.rsc.org/chemcomm

COMMUNICATION

Crystal-like microporous hybrid solid nanocast from Cr-MIL-101†

Yan Meng,[a] Guang-Hui Wang,[b] Stephan Bernt,[c] Norbert Stock*[c] and An-Hui Lu*[b]

Received 21st June 2011, Accepted 29th July 2011
DOI: 10.1039/c1cc13699b

A crystal-like ordered microporous inorganic hybrid solid was prepared using silane functionalized Cr-MIL-101 (Si-MIL-101) as the precursor, *via* a surface coating reinforced framework strategy.

In the past years, various ordered micro-, meso- and macroporous solids have been successfully replicated using the nanocasting approach.[1] Particularly, for those solids that are difficult to prepare *via* solution phase surfactant templating, the nanocasting approach provides a promising route for the preparation of ordered porous materials with novel framework compositions. Very few successful examples of nanocasting of microporous materials, other than ordered mesoporous and macroporous solids, have been demonstrated. These are limited to zeolite Y[2] and zeolite EMC-2.[3]

Crystalline porous metal–organic frameworks (MOFs) are constructed from inorganic bricks, often metal-oxygen clusters, and organic moieties.[4,5] Their porosities are mostly in the microporous to lower mesoporous range.[6] Owing to their versatile structures and compositions, MOFs may be very interesting precursors for nanocasting of other hybrid porous solids. However, to the best of our knowledge, no ordered microporous solid has been nanocast from MOFs. The only reported example to nanocast carbon from MOF-5 resulted in a highly porous, but X-ray amorphous material.[7] That is probably due to the inferior thermal stability of MOF-5 compared to silica- and carbon-based porous materials.

Herein, we present a surface coating reinforced framework strategy for the preparation of ordered microporous solids *via* the nanocasting method using Cr-MIL-101[6g,8] as the template. The structure of Cr-MIL-101 has two types of mesoporous cavities with free diameters of *ca.* 2.9 and 3.4 nm accessible through two microporous windows of *ca.* 1.2 and 1.6 nm, and a large number of unsaturated chromium sites (*ca.* 3.0 mmol g^{-1}). Through coordination of 3-aminopropyltriethoxysilane (APTES) to unsaturated chromium sites and the π–π interaction between resorcinol and terephthalate, the replica inherits the octahedral crystal-shape and the ordered structure of the template Cr-MIL-101 after pyrolysis. Moreover, the metal species are still highly dispersed in the skeleton of the product.

First, the as-synthesized Cr-MIL-101 was functionalized with APTES.[8a] For simplicity, the functionalized template is denoted by **A** in the following context. The greenish powder was evacuated at 150 °C overnight to remove adsorbed solvent molecules. Subsequently, an ethanolic solution of resorcinol of defined concentration was introduced into the pores of **A** *via* the incipient wetness technique. After removal of the ethanol, polymerization was carried out in the presence of paraformaldehyde under Ar to form composites, denoted by **A**-P-*x*, where P and *x* indicate the polymeric state and the concentration of resorcinol, respectively. The composites were converted to microporous replicas, denoted by **A**-C-*x*, by pyrolysis at 650 °C under an Ar atmosphere.

The maximum amount of resorcinol (20%) was calculated based on its density and the pore volume of template **A**, by assuming the pores of the template being completely filled. After polymerization (Fig. 1a, **A**-P-20), only small changes in

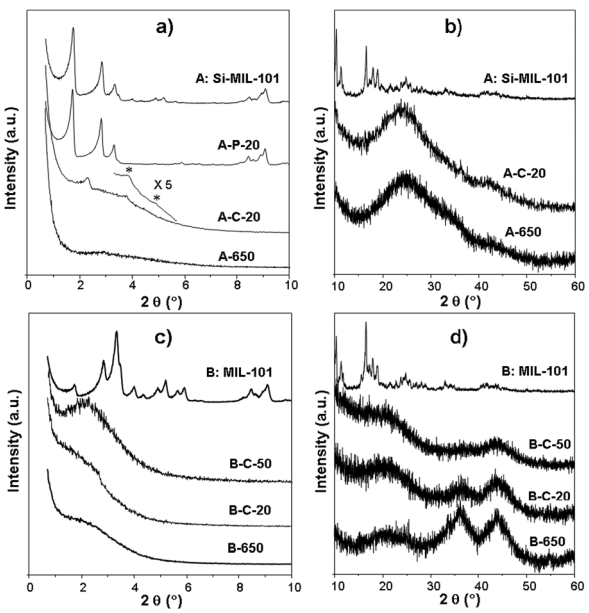

Fig. 1 (a) Low-angle XRD patterns of template **A** (silane functionalized Cr-MIL-101), **A**-P-20, **A**-C-20 and **A**-650 (template **A** pyrolyzed at 650 °C), (b) wide-angle XRD patterns of **A**, **A**-C-20 and **A**-650, (c and d) XRD patterns of template **B** (Cr-MIL-101) and the carbonized samples (**B**-C-20, **B**-C-50 and **B**-650).

[a] *Max-Planck-Institut für Kohlenforschung, Kaiser-Wilhelm-Platz 1, D-45470, Mülheim an der Ruhr, Germany*
[b] *State Key Laboratory of Fine Chemicals, School of Chemical Engineering, Dalian University of Technology, Dalian 116024, China. E-mail: anhuilu@dlut.edu.cn*
[c] *Institut für Anorganische Chemie, Christian-Albrechts-Universität zu Kiel, Max-Eyth Str. 2, D-24118 Kiel, Germany. E-mail: stock@ac.uni-kiel.de*

† Electronic supplementary information (ESI) available: Experimental details, Fig. S1–S2 and Table S1. See DOI: 10.1039/c1cc13699b

the XRD peak intensities and positions can be observed, indicating the stability of the periodical structure of Cr-MIL-101. Combined with results from nitrogen sorption measurements (Fig. 4), we suggest that the polymer RF coats the internal surface of **A** *via* π–π interaction between resorcinol and terephthalate ions. The low-angle XRD pattern of **A**-C-20 (Fig. 1a) exhibits three small but visible diffraction peaks at 2.3, 3.7 and 4.4°, corresponding to those at 1.7, 2.8, and 3.3° in the XRD pattern of template **A**. This implies the successful replication of the periodic structure of Cr-MIL-101. The XRD peaks shift to higher 2θ values due to thermal shrinkage of the structure after pyrolysis. In order to examine the function of the coated polymer, template **A** was directly pyrolyzed at 650 °C (named as **A**-650). Its XRD pattern shows no clear reflections, indicating that the coating of the polymer is indispensable for retaining the ordered structure. When increasing the loading amount of resorcinol to 50% and 80%, the low-angle XRD patterns of the products were weak and only a broad reflection was observed (Fig. S1a, ESI†). In addition, the larger amounts of resorcinol resulted in an excess amount of carbon on the outside of the replicated crystals (Fig. S1b, ESI†).

The high-resolution SEM images (Fig. 2) of the ordered replica **A**-C-20 exhibit the same crystal morphology as its parent Cr-MIL-101, but a rougher surface. This indicates that the current synthetic strategy is suitable for retaining the crystal shape of the Cr-MIL-101 template, which was not possible in nanocasting of MOF-5.[7] The STEM image (Fig. 3a) shows the octahedral morphology of **A**-C-20 crystals, which is consistent with the SEM results. Moreover, it can be clearly seen that the **A**-C-20 crystals are facetted. Cross-like dark contrast lines (Bragg fringes) divide the facetted surface according to the projected symmetry along the electron beam. The [111] oriented crystal shows hexagonal facets and the Bragg fringes draw a perfect six-fold star. The rectangle shaped particle corresponds to a [112] oriented cubic crystal. A long-range regularity can be observed in the whole particle domain of **A**-C-20 as shown in Fig. 3b and c. The electron diffraction pattern in Fig. 3c confirms the ordered pore structure within the crystal. The high resolution STEM image in Fig. 3d clearly shows the micropores with sizes of ~1 nm. No large Cr-containing crystals are observed, suggesting that the chromium is finely dispersed in the hybrid material. This is further proved by element mapping using energy dispersive X-ray spectroscopy (EDXS) (Fig. 3e). The schematic representation of TEM images along [111] and [112] is given in Fig. 3f. This phenomenon has been reported for Cr-MIL-101.[9]

The FT-IR spectrum of **A**-C-20 exhibits relative broad bands, and the bands corresponding to organic polymer

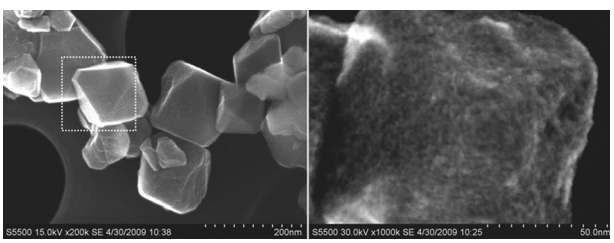

Fig. 2 SEM images of crystal-like microporous hybrid solid **A**-C-20.

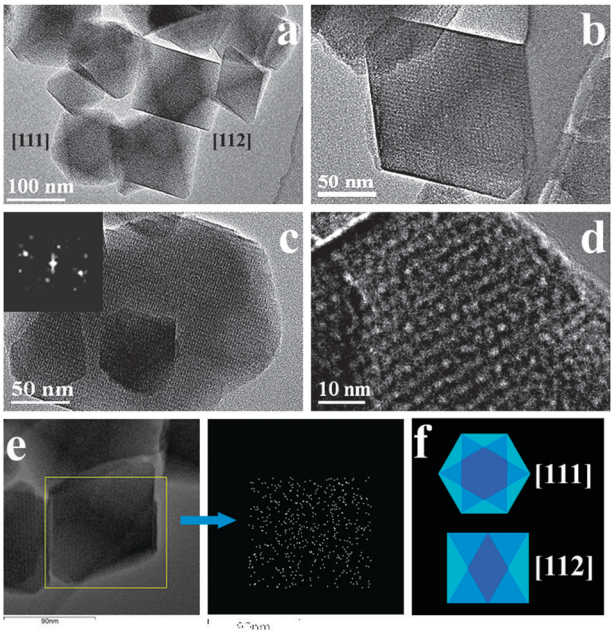

Fig. 3 STEM images (a, b, c and d) of crystal-like microporous replica **A**-C-20; energy dispersive X-ray (EDX) mapping (e) of Cr in **A**-C-20; and schematic representations of TEM images (f) of **A**-C-20 along [111] and [112]. The scale bar in e is 90 nm.

disappear (Fig. S2, ESI†). This suggests that **A**-C-20 is mainly composed of carbon and some inorganic material. In addition, the XRD pattern of **A**-C-20 (Fig. 1b) shows broad reflections in the 2θ range from 20° to 35°, indicating this material is essentially amorphous at the atomic scale. Noticeably, no reflections corresponding to chromium oxides were observed. However, the EDX measurement reveals that **A**-C-20 contains 22 wt% of Cr (Table S1, ESI†). These results suggest that the Cr species form small nanoparticles or clusters, which is consistent with the STEM results. Resembling **A**-C-20, the XRD pattern of **A**-650 (Fig. 1b) shows no reflections corresponding to Cr-containing species. This suggests that the silane functional groups hinder the agglomeration of coordinated chromium ions at high temperature and favors a high dispersion of Cr-based species.

For comparison, the as-synthesized Cr-MIL-101 without silane functionalization (named as **B**, products from **B** were denoted by **B**-C-*x*, here C and *x* have the same meaning as that of A series samples) was used as a template. As shown in Fig. 1c, the XRD patterns of pyrolyzed samples **B**-C-20 and **B**-C-50 show broad reflection with low intensity in the 2θ range of 1° to 4°, which indicate that it is rather difficult to obtain an exact replica using the Cr-MIL-101 template. The wide-angle XRD pattern (Fig. 1d) of B-650 (**B** pyrolyzed at 650 °C) and **B**-C-20 exhibits broad reflections in the 2θ range of 30° to 50°, which could be assigned to Cr_3C_2 [JCPSD 65-897] and Cr_7C_3 [JCPSD 65-1347]. Increasing the loading amount to 50% (**B**-C-50), these reflections are still visible even though they become weak. These suggest a nanocrystalline nature of the Cr species in the products. On the basis of the above-mentioned results from the two series of samples **A**-C-*x* and **B**-C-*x*, one can conclude that a silane modified template is suitable for the replication of ordered structure of Cr-MIL-101.

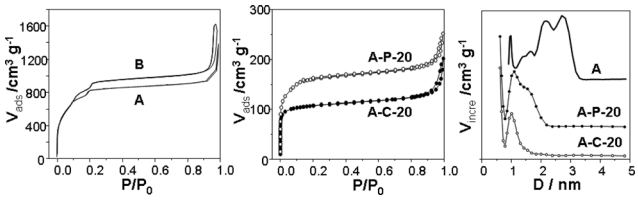

Fig. 4 N_2 sorption isotherms of templates **A** and **B**, A-P-20 and **A**-C-20; NLDFT pore size distributions of **A**, **A**-P-20 and **A**-C-20.

Thus, the silane functional groups not only stabilize the Cr ions but also help resorcinol to reinforce the Cr-MIL-101 framework.

The sorption isotherms (Fig. 4) of **A** and **B** are almost identical in shape, indicating that the small mesopores were not blocked by the functionalization with APTES. The nitrogen uptake of **A** decreased slightly compared to **B**, due to the introduction of the silane. After polymer coating and pyrolysis, the nitrogen sorption isotherm of **A**-P-20 and **A**-C-20 are essentially of type I, revealing predominantly a microporous feature. The hysteresis at $P/P_0 > 0.9$ corresponds to the condensation of nitrogen in the pores between the particles, *i.e.* the textural porosity. The disappearance of the small step at relative pressure $P/P_0 = 0.1$–0.2 in the isotherms indicates that the small mesopores were reduced in size after surface coating of the polymer on the skeleton of the template. This result is consistent with the pore size distribution calculated using the NLDFT method (Fig. 4). The NLDFT pore size distribution curve of the template **A** has maxima at 2.7, 2.2, 1.6 and 0.98 nm. After polymer coating, the NLDFT pore size distribution curve of **A**-P-20 exhibits a remarkable decrease in mesopore size and is mainly concentrated at 1.5 and 1.1 nm. After pyrolysis, sample **A**-C-20 exhibits a dominant micropore size of 1.0 nm which is in good agreement with the STEM observations. The specific surface area and total pore volume of **A**-C-20 are 363 $m^2\ g^{-1}$ and 0.24 $cm^3\ g^{-1}$, respectively. The BET surface area and the total pore volume of **A**-P-20 are calculated to be 557 $m^2\ g^{-1}$ and 0.29 $cm^3\ g^{-1}$, respectively. Together with the XRD result, we suggest that the polymer coats on the internal surface of template **A**. As the loading amount of resorcinol increases to 50%, **A**-P-50 has a very low surface area of 33 $m^2\ g^{-1}$ because of the pore blocking by an excess amount of polymer. Moreover, the XRD result of **A**-C-50 indicates that the ordered structure is not preserved. Thus, the coating instead of the filling strategy is important for successful replication of a MOF structure.

In conclusion, we have established a method for the replication of the ordered nanostructure of the MOF Cr-MIL-101 by a surface coating reinforced framework strategy. Low degrees of loading and aminosilane functionalization have shown to be crucial and successful for the replication of Cr-MIL-101. The latter suppresses the formation of larger Cr-containing particles. To the best of our knowledge, this is the first example for the successful preparation of ordered microporous crystals from MOF-like structures. This could provide a versatile way to inorganic hybrid materials with ordered microporous structures and embedded, highly dispersed metal-containing species.

We would like to thank the Fundamental Research Funds for the Central Universities and the Program for New Century Excellent Talents in University of China (NECT-09-0254). We thank Mr Spliethoff and Mr Bongard for TEM and SEM measurements.

Notes and references

1 (*a*) F. Schüth, *Angew. Chem., Int. Ed.*, 2003, **42**, 3604; (*b*) R. Ryoo, S. H. Joo, M. Kruk and M. Jaroniec, *Adv. Mater.*, 2001, **13**, 677; (*c*) H. Yang and D. Zhao, *J. Mater. Chem.*, 2005, **15**, 1217; (*d*) A.-H. Lu and F. Schüth, *Adv. Mater.*, 2006, **18**, 1793; (*e*) C. D. Liang, Z. J. Li and S. Dai, *Angew. Chem., Int. Ed.*, 2008, **47**, 3696; (*f*) A. Stein, Z. g. Wang and M. A. Fierke, *Adv. Mater.*, 2009, **21**, 265; (*g*) A.-H. Lu, D. Zhao and Y. Wan, *Nanocasting: A Versatile Strategy for Creating Nanostructured Porous Materials*, Royal Society of Chemistry, 2009; (*h*) Z. Zhang, F. Zuo and P. Feng, *J. Mater. Chem.*, 2010, **20**, 2206.

2 (*a*) T. Kyotani, T. Nagai, S. Inoue and A. Tomita, *Chem. Mater.*, 1997, **9**, 609; (*b*) J. Rodriguez-Mirasol, T. Cordero, L. R. Radovic and J. J. Rodriguez, *Chem. Mater.*, 1998, **10**, 550; (*c*) S. A. Johnson, E. S. Brigham, P. J. Ollivier and T. E. Mallouk, *Chem. Mater.*, 1997, **9**, 2448.

3 (*a*) F. O. M. Gaslain, J. Parmentier, V. P. Valtchev and J. Patarin, *Chem. Commun.*, 2006, 991; (*b*) T. Roussel, A. Didion, R. J. M. Pellenq, R. Gadiou, C. Bichara and C. Vix-Guterl, *J. Phys. Chem. C*, 2007, **111**, 15863.

4 (*a*) G. Férey, *Chem. Soc. Rev.*, 2008, **37**, 191; (*b*) S. Kitagawa, R. Kitaura and S.-I. Noro, *Angew. Chem., Int. Ed.*, 2004, **43**, 2334; (*c*) P. Horcajada, T. Chalati, C. Serre, B. Gillet, C. Sebrie, T. Baati, J. F. Eubank, D. Heurtaux, P. Clayette, C. Kreuz, J.-S. Chang, Y. K. Hwang, V. Marsaud, P.-N. Bories, L. Cynober, S. Gil, G. Ferey, P. Couvreur and R. Gref, *Nat. Mater.*, 2010, **9**, 172; (*d*) O. M. Yaghi, M. O'Keeffe, N. W. Ockwig, H. K. Chae, M. Eddaoudi and J. Kim, *Nature*, 2003, **423**, 705.

5 (*a*) M. Eddaoudi, J. Kim, N. Rosi, D. Vodak, J. Wachter, M. O'Keeffe and O. M. Yaghi, *Science*, 2002, **295**, 469; (*b*) S. Surble, C. Serre, C. Mellot-Draznieks, F. Millange and G. Férey, *Chem. Commun.*, 2006, 284.

6 (*a*) N. Klein, I. Senkovska, K. Gedrich, U. Stoeck, A. Henschel, U. Mueller and S. Kaskel, *Angew. Chem., Int. Ed.*, 2009, **48**, 9954; (*b*) K. Koh, A. G. Wong-Foy and A. J. Matzger, *J. Am. Chem. Soc.*, 2009, **131**, 4184; (*c*) K. Koh, A. G. Wong-Foy and A. J. Matzger, *Angew. Chem., Int. Ed.*, 2008, **47**, 677; (*d*) H. K. Chae, D. Y. Siberio-Perez, J. Kim, Y. B. Go, M. Eddaoudi, A. J. Matzger, M. O'Keeffe and O. M. Yaghi, *Nature*, 2004, **427**, 523; (*e*) D. Sun, S. Ma, Y. Ke, D. J. Collins and H.-C. Zhou, *J. Am. Chem. Soc.*, 2006, **128**, 3896; (*f*) R. Banerjee, A. Phan, B. Wang, C. Knobler, H. Furukawa, M. O'Keeffe and O. M. Yaghi, *Science*, 2008, **319**, 939; (*g*) G. Férey, C. Mellot-Draznieks, C. Serre, F. Millange, J. Dutour, S. Surblé and I. Margiolaki, *Science*, 2005, **309**, 2040; (*h*) A. Sonnauer, F. Hoffmann, M. Fröba, L. Kienle, V. Duppel, M. Thommes, C. Serre, G. Férey and N. Stock, *Angew. Chem., Int. Ed.*, 2009, **48**, 3791; (*i*) D. Yuan, D. Zhao, D. J. Timmons and H.-C. Zhou, *Chem. Sci.*, 2011, **2**, 103.

7 B. Liu, H. Shioyama, T. Akita and Q. Xu, *J. Am. Chem. Soc.*, 2008, **130**, 5390.

8 (*a*) Y. K. Hwang, D.-Y. Hong, J.-S. Chang, S. H. Jhung, Y.-K. Seo, J. Kim, A. Vimont, M. Daturi, C. Serre and G. Férey, *Angew. Chem., Int. Ed.*, 2008, **47**, 4144; (*b*) Y. Pan, B. Yuan, Y. Li and D. He, *Chem. Commun.*, 2010, **46**, 2280.

9 O. I. Lebedev, F. Millange, C. Serre, G. Van Tendeloo and G. Ferey, *Chem. Mater.*, 2005, **17**, 6525.